Elsevier Editorial System(tm) for Scripta Materialia

Manuscript Draft

Manuscript Number: SMM-18-1347R1

Title: Core-shell structure: an effective feature for strengthening ZrB2 ceramics

Article Type: Regular article

Keywords: borides; core-shell; creep; dislocation mobility; grain boundaries.

Corresponding Author: Dr. Laura Silvestroni,

Corresponding Author's Institution: CNR

First Author: Laura Silvestroni

Order of Authors: Laura Silvestroni; Simone Failla; Vladimir Vinokurov; Irina Neshpor; Oleg Grigoriev

Abstract: Hot compression behavior of two ZrB2 ceramics containing SiC or WSi2 particles was investigated upon stepwise heating from 1700 to 2100°C under static load in vacuum. Presence of SiC activated notable creep already at 1700°C, owing to diffused silica softening at SiC/SiC interfaces, whilst for WSi2 appreciable deformation occurred only above 1900°C. Limited amount of SiC particles, which is responsible for cavitation, and formation of (Zr,W)B2 solid solution, able to accommodate high mechanical loads through plastic deformation, are fundamental characteristics to remarkably perform in hot environments. Particularly, dislocation activity in the solid solution plays a fundamental role at ultra-high temperatures.

National Research Council of Italy
istec Institute of Science and Technology for Ceramics

Faenza, July 13th 2018

COVER LETTER

Dear Editor in Chief,

please find the manuscript "Core-shell structure as key for ultra-refractory ZrB_2 ceramics".

This manuscript is focused on the microstructure evolution of two ultra-high temperature ceramics which underwent hot compression up to 2100°C under static load in vacuum. The effect of the addition of 15 vol% of WSi_2 is compared to that of SiC particles added in the same amount within a ZrB_2 matrix.

Presence of SiC activated notable creep already at 1700°C, owing to diffused silica softening at SiC/SiC interfaces, whilst for WSi_2 appreciable deformation occurred only above 1900°C. Limited amount of SiC particles, responsible for cavitation, and formation of $(Zr,W)B_2$ solid solution, able to accommodate high mechanical loads through plastic deformation, are fundamental characteristics to remarkably perform in hot environments. Particularly, dislocation activity in the solid solution plays a fundamental role at ultra-high temperatures.

In this work we noticed for the first time misalignment between core and shell upon hot compression test, suggesting different response to the mechanical load.

We hope that this paper will meet the high standards for publication in *Scripta Materialia*.

Yours sincerely,

Laura Silvestroni

National Research Council of Italy
istec Institute of Science and Technology for Ceramics

Faenza, September 22nd 2018

RESPONSE TO REVIEWERS' COMMENTS

Dear Editor in Chief,
We are very grateful to the referee for the useful comments and suggestions on our manuscript originally entitled "Core-shell structure as key for ultra-refractory ZrB2 ceramics" (SMM-18-1347).
All the comments have been addressed and the manuscript has been carefully revised. All the changes are marked in red in the revised file and a summary of the contents revision is reported here below.

Reviewer #1: It is a nice manuscript on the deformation behavior of ZrB2-SiC and ZrB2-WSi2 ceramics during a stepwise heating. The interesting property was related with the microstructural features of these ceramics, especially for the core-shell structure and dislocation. Some detailed comments are shown below to improve the quality of the work.

1. For the title, it is a bit broad. After reading it, the reviewer had no idea about the scope of the paper. Core-shell structures in borides had been found in lots of compositions. The title should be concise, focusing on the specific topic in this work.
The title has been changed accordingly into "Core-shell structure: an effective feature for strengthening ZrB_2 ceramics".

2. In the abstract, the condition of hot deformation is unclear. "Hot compression behavior of two ZrB2 ceramics containing SiC or WSi2 particles was investigated in the 1700-2100°C temperature range under static load in vacuum". Without looking through the text, it seems that the deformation was investigated at different temperatures between 1700-2100oC. In fact, the investigation was based on a stepwise heating. Again, it should be documented precisely.
We defined more clearly the test conditions in the abstract, evidenced in red.

3. In the experimental parts, the averaged particle size of ZrB2 particle should be documented. 0.1-6 micro is too broad. Why a mild load of 48MPa was adopted in this study? If two graphite pistons were used to deform the diboride cylinder, did you consider the deformation/expansion of graphite during heating? If not, the displacement curve in Fig.2a will be inaccurate. From my point of view, graphite should be easily deformed compared with diboride, the major contribution on the displacement should be caused by the pistons. On the characterization part, many images in the manuscripts have not been labelled clearly, it is difficult to know whether they were collected by SEM, TEM or STEM, just from the figure captions.
ZrB_2 powder size details have been added including d_{90}, d_{50}, d_{10}.
The applied load, 48 MPa, is the maximum allowed by the testing set-up.
The expansion of the graphite pistons has been of course considered and the ΔL corrected accordingly. generally, the ΔL due to pistons compression is in the order of 0.1 mm.
We reported in the figure captions whether the image was taken by SEM or TEM to avoid misunderstanding, evidenced in red.

4. "different grey levels of the matrix in SEM imaging are due to different grains orientation" Can it be caused by the composition difference? Actually, the contrast of ZrB2 grains is not very clear in Fig.1.
It is correct, both grain orientation and composition influence the contrast in SEM imaging. However, the boride grains in ZS consist of pure ZrB_2 without cation impurities, therefore contrast variations are only due to different orientation. Using the visualization conditions adopted for the ZS sample in Fig. 1a

the grain boundary is not too clear, but in order to have a proper contrast between SiC and ZrB_2 and provide a representative material overview we had to sacrifice the grain boundary aspect.

5. Dislocation study in TEM should be done in a two-beam condition. The direction of g vector should be labelled in the corresponding images. It applies for Fig. 1b, 2b and 2c.
Yes, it is right, but since in this work we did not speculate on the g·b analysis of dislocations, we do not think it is a necessary information.

6. In Figure 3b and c, could you explain it further, which is the slip plane for the dislocation array and their corresponding Burgers vector? I guess <a> type dislocation should be activated due to the smaller magnitude of b.
Same as above, in this work we qualitatively present dislocation arrays without quantitative speculation, therefore we omitted this parameter in order to avoid overloading with non-necessary information.

7. It is OK to observe and analyse the dislocation by SEM (BSE) through an ECCI contrast. However, the condition to get such images in Fig.4 should be clarified (How did you tilt the sample? How did you confirm the grain orientation, possibly by EBSD? g vector under two beam condition used in this work, the working distance and voltage to achieve such images, is it a normal BSE detector or an in-lens one). See the reference: Philosophical Magazine Volume 97, Issue 5, 11 February 2017, Pages 346-359. Without putting such detailed parameters, it is hard to perform similar work at the other groups.
In this paper we do not quantitatively speculate on grain orientation and therefore we do not believe the information requested are necessary for the aim of the work. We adopted conventional ECCI conditions. We added the suggested reference to strengthen our findings, [24].

8. Can the limited SiO2 in ZrB2-WSi2 be caused by the in-situ formed WC in ZW? Its removal could be discussed further with referencing some recent work.
Residual silica could be due to the suggested reaction, but also to the reaction between WSi2 and the B2O3 covering surface of the diboride particles yelding WB, Si and SiO2 [ref. 17]. We added the reaction and corresponding reference, [21].

9. There is a recent paper on the strengthening of ZrB2 based ceramics at high temperatures via dislocation strengthening, it should be kindly cited. Segregation of W at the grain boundary of boride may also exist in this system, together with the core-shell structure. Scripta Materialia, Volume 157, December 2018, Pages 76-80.
Thank you very much for the indication of this interesting very recent paper which I could not yet read at the time of this initial submission. We added this reference, [28].

We hope that our manuscript in its revised form will meet the high standard for publication in Scripta Materialia.

Yours sincerely,
Laura Silvestroni

*Graphical Abstract

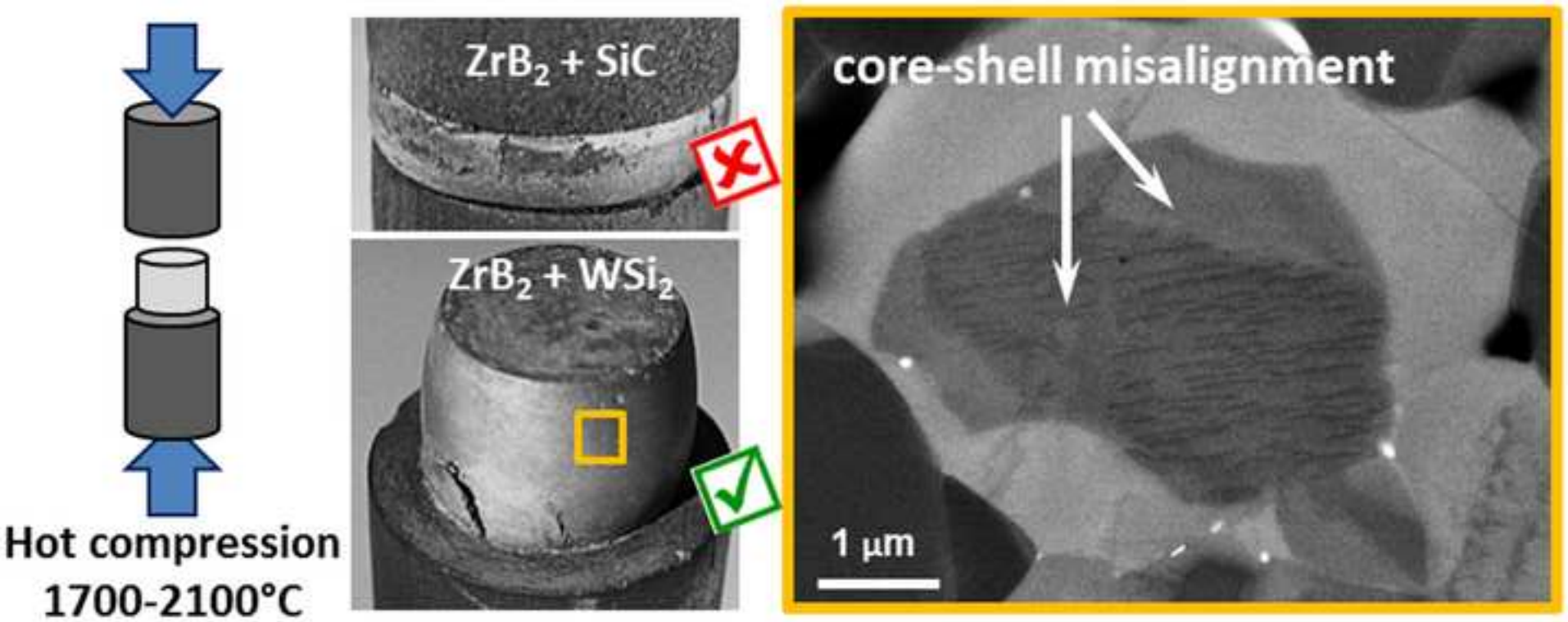

Core-shell structure: an effective feature for strengthening ZrB_2 ceramics

Laura Silvestroni[11], Simone Failla[1,2], Vladimir Vinokurov[3], Irina Neshpor[3], Oleg Grigoriev[3]

[1]CNR-ISTEC, National Research Council of Italy - Institute of Science and Technology for Ceramics, Via Granarolo 64, 48018 Faenza, Italy

[2]University of Parma, Department of Chemistry, Life Science and Environmental Sustainability, Parco Area della Scienza 11/a, 43124 Parma, Italy

[3]IPMS, Frantsevich Institute for Problems of Materials Science NAS of Ukraine, 3 Krzhizhanovskoho St., 03680 Kyev, Ukraine

ABSTRACT

Hot compression behavior of two ZrB_2 ceramics containing SiC or WSi_2 particles was investigated upon stepwise heating from 1700 to 2100°C under static load in vacuum. Presence of SiC activated notable creep already at 1700°C, owing to diffused silica softening at SiC/SiC interfaces, whilst for WSi_2 appreciable deformation occurred only above 1900°C. Limited amount of SiC particles, which is responsible for cavitation, and formation of $(Zr,W)B_2$ solid solution, able to accommodate high mechanical loads through plastic deformation, are fundamental characteristics to remarkably perform in hot environments. Particularly, dislocation activity in the solid solution plays a fundamental role at ultra-high temperatures.

Keywords: borides; core-shell; creep; dislocation mobility; grain boundaries.

stepwise heating

Main body

Ultra-high temperature ceramics (UHTCs) are materials intended for temperatures exceeding 1600°C, owing to their melting point above 3000°C and excellent thermo-mechanical properties [1]. In the last decades, many studies have been concentrated on the amelioration of processing conditions, mechanical performances and oxidation resistance [1–7], but only a limited number of them is focused on the actual target temperature range where these materials are envisioned to operate [8,9]. In particular, creep and deformation behaviour are limited to the 1425-1600°C temperature range [10–12], whilst investigations at higher temperatures are rather unexplored but necessary to validate UHTC response in extreme environments. Most of the creep studies investigated ZrB_2 coupled with SiC, ZrN and Si_3N_4, which are common secondary phases used to promote densification [13], enhance the oxidation resistance and the mechanical properties [14,15]. It has been shown that a reduction of ZrB_2 grain size or of any secondary phase of the composite and an increase of SiC volume fraction accelerate creep mechanism, owing to higher fraction of interfacial glassy phase that enhances grain-boundary sliding and formation of cavities at the particle-matrix interfaces [10,16]. However SiC, or some SiO_2 precursor, is needed when these materials are exposed to oxidizing environments at moderate temperatures, since it enables the formation of a passivating silico-borate glass on the outermost

[1] Corresponding author: Laura Silvestroni
Tel. +39 546 699723
Fax. +39 546 46381
e-mail. laura.silvestroni@istec.cnr.it

surface. The introduction of refractory secondary phases, possibly a transition metal silicide, able to pin the grains sliding at high temperature and to form a passivating oxide layer, could be a sound strategy to limit deformation and creep mechanisms and protect from oxygen attack.

In this work, we compare the hot compression behaviour upon stepwise heating from 1700 to 2100°C under static load in vacuum atmosphere of two ZrB_2-based composites: a reference containing 15 vol% of SiC particles (ZS), and another one initially batched with the same amount of WSi_2 phase (ZW). This silicide has been selected in view of its proved beneficial effect on the mechanical properties, like strength retention of 84% at 1500°C in air [17,18] and moderate oxidation up to 1650°C [19].

The following commercial powders were used to prepare the ceramic pellets: hexagonal ZrB_2, Grade B (H.C. Starck, Germany), specific surface area 1.0 m^2/g, impurity max content: C: 0.25 wt%, O: 2 wt%, N: 0.25 wt%, Fe: 0.1 wt%, Hf: 0.2 wt%, particle size range 0.1-6 µm with d_{10}: 0.6 µm, d_{50}: 2.3 µm, d_{90}: 4 µm; hexagonal SiC (Enomaterial, China), mean grain size 0.5 µm, 99.9%, impurity max content: 0: 0.1 wt%; tetragonal WSi_2, (Sigma Aldrich, Milano, Italy), -325 mesh, 99.5%, traces of metals <6000 ppm. The powder mixtures were ball milled with zirconia media in a polyethylene jar for 24 h in absolute ethanol at 130 rpm. Subsequently the slurries were dried in a rotary evaporator. Sintering was conducted in a hot pressing furnace in low vacuum (~100 Pa) using an induction-heated graphite die with a constant uniaxial pressure of 30 MPa, heating rate 20°C/min and free cooling. The maximum sintering temperature was 1930°C for both composites. The bulk density was measured by Archimedes' method.

Cylindrical specimens, 8 mm in diameter and 10 mm in height, were machined from the sintered billets and subjected to hot compression tests under constant load of 48 MPa in vacuum atmosphere in the 1700-2000°C temperature range. Each sample was mounted between two graphite pistons and heated to 1700°C with a heating rate of 500°C/min. Temperature increment of 50°C was set from 1700 to 2100°C. Each temperature was maintained for 15 minutes to enable the achievement of the thermal equilibrium and then heating was moved forward to the next target temperature. Control of the sample deformation was continuously monitored through linear movement of the upper ram displacement.

The microstructure before and after hot compression was analyzed on polished cross-sections by field-emission scanning electron microscopy (FESEM, mod. ΣIGMA, ZEISS NTS Gmbh, Germany) coupled to an energy dispersive X-ray micro-analyzer (EDS, mod. INCA Energy 300, Oxford Instruments, UK). Specimens for TEM analyses were prepared by cutting a disc from selected samples. The discs were mechanically ground down to about 20 µm and then further ion beam thinned until incipient perforations were observed by optical microscope. Local phase analysis was performed using a transmission electron microscope (TEM, JEOL JEM 2100F) operating at a nominal voltage of 200 kV and equipped with an energy-dispersive X-ray system (EDS, mod. INCA Energy 300, Oxford instruments, UK).

Key microstructural features, like residual porosity, mean grain size and volumetric content of the secondary phases, were evaluated from FESEM micrographs elaborated with the support of the commercial software package Image Pro Plus (v.7, Media Cybernetics, USA).

SEM analysis of the as-sintered materials revealed fully dense ceramics without macro defects. In both cases, the diboride matrix was spatially uniform with mean grain size around 2-3 µm, different grey levels of the matrix in SEM imaging are due to different grains orientation.

ZS baseline had homogeneously dispersed SiC particles, with agglomerate size of 3-5 µm, Fig. 1a. Residual SiO_2 pockets with irregular profiled shape were trapped within SiC aggregates as reaction by-products with oxides covering the

powders during sintering [20,21].

ZW material was more clean from secondary phases and the boride matrix developed a sub-structure commonly known as “core-shell”, in which grains are comprised of a stoichiometric ZrB_2 core surrounded by an isostructural $(Zr,W)B_2$ solid solution shell, Fig. 1b. The amount of W in the shell was in the range of 2–4 at%, as detected by EDS, and the shell comprised ~30% of the volume of the ZrB_2-based matrix, based on image analysis estimation on polished surfaces. A peculiar feature of the matrix grains was the presence of dislocations in the shell, as visible by TEM in the inset of Fig. 1b. Similarly to previous study on analogous composites [17,22], core and shell were epitaxial and the boundary between the two zones was quite sharp and defined by dislocations pile up. Further, analyses of the interfaces revealed non wetted grain boundaries between boride-boride grains and boride-secondary phases [17]. Minor phases in ZW included about 2 vol% of silica, with dark contrast, and newly formed W-based compounds with white contrast, WB and a mixed (Zr,W)C phase, both at the triple points and as 2 μm discrete grains. At the triple junctions, residuals of WSi_2 with convex shape were regularly found. In addition, about 1 vol% of small SiC grains were also found next to silica pockets. All these new compounds are the result of dissociation and reaction phenomena occurring during hot pressing by reactions of the starting raw powders and/or the native oxides covering them, as extensively reported in [17,21].

The shrinkage of each cylinder was monitored during the compression tests through the upper ram movement and Fig. 2 reports the normalized height variation, ΔL, as a function of the increasing temperature versus time for the two materials with a picture of the specimens at the end of the test, still between or on the graphite pistons. It is immediately noticeable that the materials behaved in notable different ways: ZS softened and creeped resulting in a homogeneous flattening, whilst ZW assumed a barrel-like shape and underwent much more limited deformation with final fracture on one edge. This macroscopic behavior finds explanation in the compression curves, where ZS starts to deform already at 1700°C, whilst ZW only above 1900°C. The overall deformation extent at the end of the test at 2100°C is also very different, 62% for ZS and 25% for ZW.

As these tests evidenced, the introduction of considerable amount of SiC in ZS generally leads to a significant increase in creep rate as compared to our SiC-free composite, ZW, and, in addition,WSi_2 has a good influence on the creep resistance, probably owing to the formation of refractory W-based compounds at the triple junctions during sintering that pin the grains sliding, as shown later.

To further explore the reasons leading to such different behavior at high temperature, thorough microstructural analysis of the hot compressed specimens was performed.

Similar to what reported in the literature [11], the investigation of the polished hot compressed ZS cross section revealed that the diboride grains did not meaningfully changed their size, owing to the large amount of SiC particles that obstructed mass transport mechanisms by diffusion, but cavities located at ZrB_2-SiC interfaces and diffused silica glass around SiC particles were systematically found, see the inset in Fig. 1a. The high volume fraction of silica scattered throughout the microstructure is considered the major factor responsible for flattening of the cylinder during the test, which indeed starts appreciable deformation at 1700°C, i.e. the melting point of silica.

The situation was remarkably different in ZW, whose microstructure upon hot compression is depicted in Fig. 3a-c. Statistical analysis of the boride grain size before and after the test is illustrated in Fig. 3d-e, where the whole grain or only the core size are distinguished. Notwithstanding the little amount of secondary phases, the mean grain size remained around 2.7 μm, probably thanks to the presence of refractory phases at the triple junctions and

preferred diffusion mechanism across core and shell rather than coalescence between shell and shell, Fig. 3d. The same trend was found the cores, Fig. 3e: they remained around 1.7 µm, with a more flattened frequency distribution, i.e. a more negative kurtosis. As for the secondary phases, morphology and spatial distribution variation were noticed on the cross section. At the top, W-B-C phases were found as large aggregates, about 3 µm wide. Moving towards the cylinder core, triple point junctions appeared too, and at the bottom silica and SiC conglomerates with analogous size prevailed. To note the peculiar variation of the shape of the triple points which passed from convex in the as-sintered material to concave upon hot compression, as visible in the inset of Fig. 3a, probably due to local variation of chemistry at the interface with the boride grain and a different wettability behavior. The spatial distribution of the secondary phases is presumably a consequence of the temperature distribution inside the test chamber, which facilitated the accumulation of liquid phases, like silica glass, downwards. TEM investigations on this sample allowed to observe high dislocation activity, much more pronounced as compared to the as-sintered material [17] and particularly concentrated in the shell region, Fig. 3b,c. Shells formally belong to grain boundary zones in which the diffusion processes are intensified as well as the rates of high-temperature dislocation processes of crowding, which is characteristic of creep. In addition, in the grain boundary zones, in the presence of applied homogeneous stresses, there will always be a concentration of stresses, which will lead to the localization of plastic processes in the shell.

SEM observation with backscattered electron detector and high voltage enabled to identify major crystalline line defective structure in grains close to the Bragg's condition [23,24]. Examples of grains favorably oriented are reported in Fig. 4. By using channelling contrast it was possible to detect the formation a second shell around the primary core-shell substructure, Fig. 4a, suggesting dissolution of grain boundary phase and mass transport to the grain. In addition and most importantly, this imaging technique enabled to image dislocations and twinning. The most frequently observed situation is depicted in Fig. 4b, where parallel bands, about 60 nm wide, run across the entire width of the grain, i.e. a series of regularly spaced dislocations cover the shell surface. However, when the core-shell structure was cross sectioned, a slight misalignment between core and shell was systematically detected, Fig. 4c, or even loss of Bragg's condition, i.e. core and shell completely lost their epitaxy, Fig. 4d. This misalignment suggests that during compression core and shell respond in a different way to the mechanical load with the shell presumably moving easier than the core. The core/shell morphology is particularly suited to absorb energy during deformation according to the "core-mantle" model proposed by Gifkins [25], which hypothesizes that dislocation movement only occurs in the mantle region of the grain, i.e. in the region close to the grain boundaries. According to this model, during testing at elevated temperatures, dislocation accumulation in the shells enables plastic deformation through dislocation movement and accommodation of mechanical stress during loading. Secondary dislocations would interact with the pre-existing dislocations forming grids, complex tangles with high dislocation density. Each of these regions could then, in turn, act as a new obstacle to further slip. Since each slip line is stopped at another, the dislocations should tend to cluster into local regions forming cell structures, thus inducing sub-grain refinement, as previously observed in [9,11].

The beneficial effect of core and shell upon load at ultra-high temperature was already confirmed in [9], where a W-doped ZrB_2-ceramic with analogous core-shell features displayed increased dislocations activity and formation of polygonised dislocation walls in the shell to accommodate for the loading at high temperature. These features enabled that material to achieve strength over 800 MPa at 1800°C.

The above results demonstrated that the SiC content in the UHTC matrix has to be carefully controlled, absence leads to poor oxidation resistance in the 1200-1700°C temperature range, excessive amount brings to

mechanical properties decay and notable deformation at high temperatures. In addition, tailoring the boride matrix grains with suitable alloying elements that form core-shell substructures is a further trick to obtain ultra-refractory ceramics with superior performance. The core/shell structure brings a series of advantages under multiple aspects. First, it enables to keep the grain size fine, i.e. possible subsequent thermal treatments like annealing to promote toughening mechanisms are possible without matrix coarsening [26]. Then the dopant is homogeneously distributed, limiting the presence of discrete phases at the grain junctions, thus preventing possible softening at high temperature or evolution of vigorous gas phases once these materials are exposed to oxidizing environment [27]. The core-shell morphology provides benefits also on the mechanical properties, since cation segregation at grain boundaries [28] and dislocation accumulation at the interface enables plastic deformation and accommodation of high loads in the ultra-high regime [9]. Finally, the boride cell is prone to host cations of diverse nature, so multiple cation doping could lead to microstructure design and functionalization depending on the final purpose of the material.

In summary, two ZrB_2 ceramics containing 15 vol% of SiC or WSi_2 particles underwent hot compression test under static load in vacuum up to 2100°C. The substitution of SiC with WSi_2 demonstrated a drastic reduction in creep temperature and rate. The temperature at which deformation started was 1700°C in the case of SiC addition and only above 1900°C for WSi_2. The major phenomena occurring in the first case are related to diffused silica glass that leads to grain boundary sliding and cavitation at the grain junctions, whilst in the second case the boride microstructure is preserved owing to the core-shell feature which can accommodate large loads in hot regime. Directions for the design of refractory ceramics employable at ultra-high temperatures include limited amount of SiC phase and functional alloying of the matrix with suitable cations that enable the formation of core-shell substructure.

Acknowledgements

The research leading to these results has received funding from the European Community's Seventh Framework Programme (FP7/2011-2014) under grant agreement LIGHT-TPS No. 607182. C. Kübel (KIT, Germany) is greatly acknowledged for precious suggestions on SEM imaging.

References

[1] W.G. Fahrenholtz, E.J. Wuchina, W.E. Lee, Y. Zhou, Ultra-High Temp. Ceram. Mater. Extrem. Environ. Appl., John Wiley & Sons, Inc., Hoboken, New Jersey, 2014.

[2] S.Q. Guo, J. Eur. Ceram. Soc. 29 (2009) 995–1011.

[3] S.Q. Guo, T. Nishimura, T. Mizuguchi, Y. Kagawa, J. Eur. Ceram. Soc. 28 (2008) 1891–1898.

[4] P. Hu, Z. Wang, J. Eur. Ceram. Soc. 30 (2010) 1021–1026.

[5] L. Silvestroni, K. Stricker, D. Sciti, H.J. Kleebe, Acta Mater. 151 (2018) 216–228.

[6] X. hong Zhang, P. Hu, J. cai Han, L. Xu, S. he Meng, Scr. Mater. 57 (2007) 1036–1039.

[7] G. Chen, R. Zhang, P. Hu, W. Han, Scr. Mater. 61 (2009) 697–700.

[8] J. Zou, V. Rubio, J. Binner, Acta Mater. 133 (2017) 293–302.

[9] L. Silvestroni, H.-J. Kleebe, W.G. Fahrenholtz, J. Watts, Sci. Rep. 7 (2017) 40730.

[10] I.G. Talmy, J.A. Zaykoski, C.A. Martin, J. Am. Ceram. Soc. 91 (2008) 1441–1447.

[11] M. Mallik, K.K. Ray, R. Mitra, J. Am. Ceram. Soc. 97 (2014) 2957–2964.

[12] W.M. Guo, G.J. Zhang, H.T. Lin, Ceram. Int. 38 (2012) 831–835.

[13] F. Monteverde, A. Bellosi, Scr. Mater. 46 (2002) 223–228.

[14] P. Hu, X.H. Zhang, J.C. Han, X.G. Luo, S.Y. Du, J. Am. Ceram. Soc. 93 (2010) 345–349.

[15] E.W. Neuman, G.E. Hilmas, W.G. Fahrenholtz, J. Am. Ceram. Soc. 96 (2013) 47–50.

[16] I.I. Spivak, R.A. Andrievskii, V. V Klimenko, V.D. Lazarenko, Sov. Powder Metall. Met. Ceram. 13 (1974) 617–620.

[17] F. Monteverde, L. Silvestroni, Mater. Des. 109 (2016) 396–407.

[18] J. Zou, G.J. Zhang, C.F. Hu, T. Nishimura, Y. Sakka, J. Vleugels, O. Van Der Biest, J. Am. Ceram. Soc. 95 (2012) 874–878.

[19] L. Silvestroni, D. Sciti, F. Monteverde, K. Stricker, H.J. Kleebe, J. Am. Ceram. Soc. 100 (2017) 1760–1772.

[20] L. Silvestroni, D. Sciti, J. Alloys Compd. 602 (2014).

[21] J. Zou, S.K. Sun, G.J. Zhang, Y. M. Kan, P.L. Wang, T. Ohji, J. Am. Ceram. Soc. 94 (2011) 1575–1583.

[22] L. Silvestroni, H.J. Kleebe, J. Eur. Ceram. Soc. 37 (2017) 1899–1908.

[23] A.J. Wilkinson, P.B. Hirsch, Micron 28 (1997) 279–308.

[24] B. Pang, I. P. Jones, Y.L. Chiu, J.C.F. Millett, G. Whiteman, Phil. Mag. 97 (2017) 346-359.

[25] R.C. Gifkins, Metall. Trans. A 7 (1976) 1225–1232.

[26] D. Sciti, L. Silvestroni, V. Medri, S. Guicciardi, J. Eur. Ceram. Soc. 31 (2011) 2145–2153.

[27] L. Silvestroni, S. Failla, I. Neshpor, O. Grigoriev, J. Eur. Ceram. Soc. 38 (2018) 2467–2476.

[28] G.J. Zou. H.B. Ma, J. Zou, J.T. Zhu, L.F. Liu, Scr. Mater. 157 (2018) 76–80.

Figures captions

Fig. 1: SEM images of the polished surface of a) as-sintered ZS with inset a detail of the SiO_2 formation upon hot compression at SiC/SiC interface, and b) as-sintered ZW evidencing SiO_2 and W-based secondary phases. The inset in b) is a TEM image showing the core-shell structure with dislocations.

Fig. 2: Plot of the shrinkage behavior as a function of time and temperature during hot compression of ZrB_2-based composites with picture of the specimens at the end of the test on the right.

Fig. 3: a) SEM image of the microstructure of ZW upon hot compression highlighting the variation of the triple junctions with concave shape in the inset. b)-c) TEM images of the boride grains evidencing dislocation activity and slip planes pointed by the arrow. Frequency distribution of d) grains and e) cores size in ZW in the as-sintered microstructure and upon hot compression.

Fig. 4: SEM images of ZW upon hot compression test showing a) the formation of a secondary shell, b)-d) dislocations running across the matrix grains. Arrows evidence complete misalignment between core and shell, i.e. loss of Bragg's condition.

Figure 1

Click here to download high resolution image

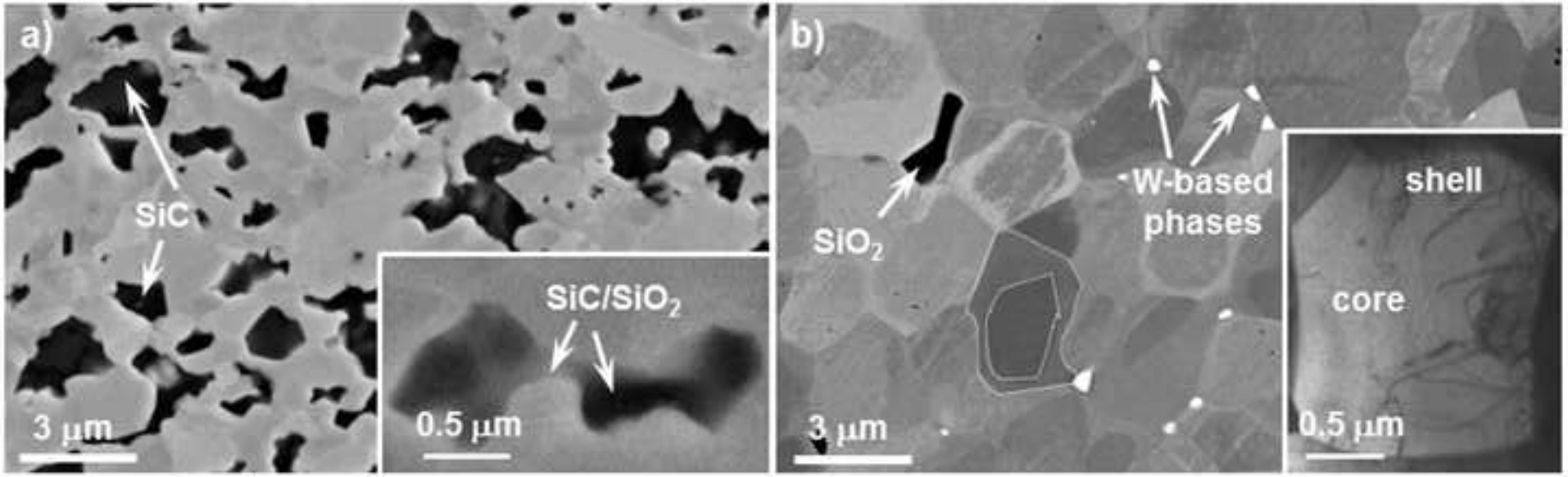

Figure 2

Click here to download high resolution image

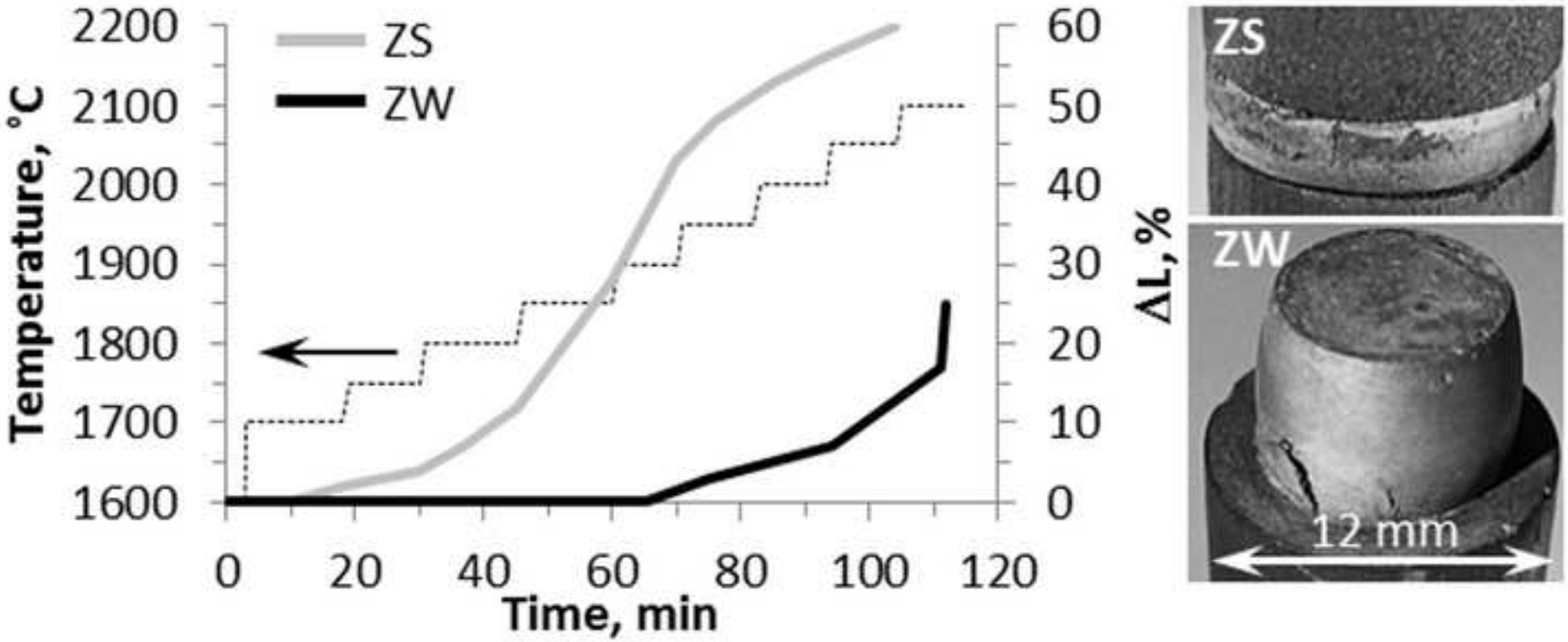

Figure 3

Click here to download high resolution image

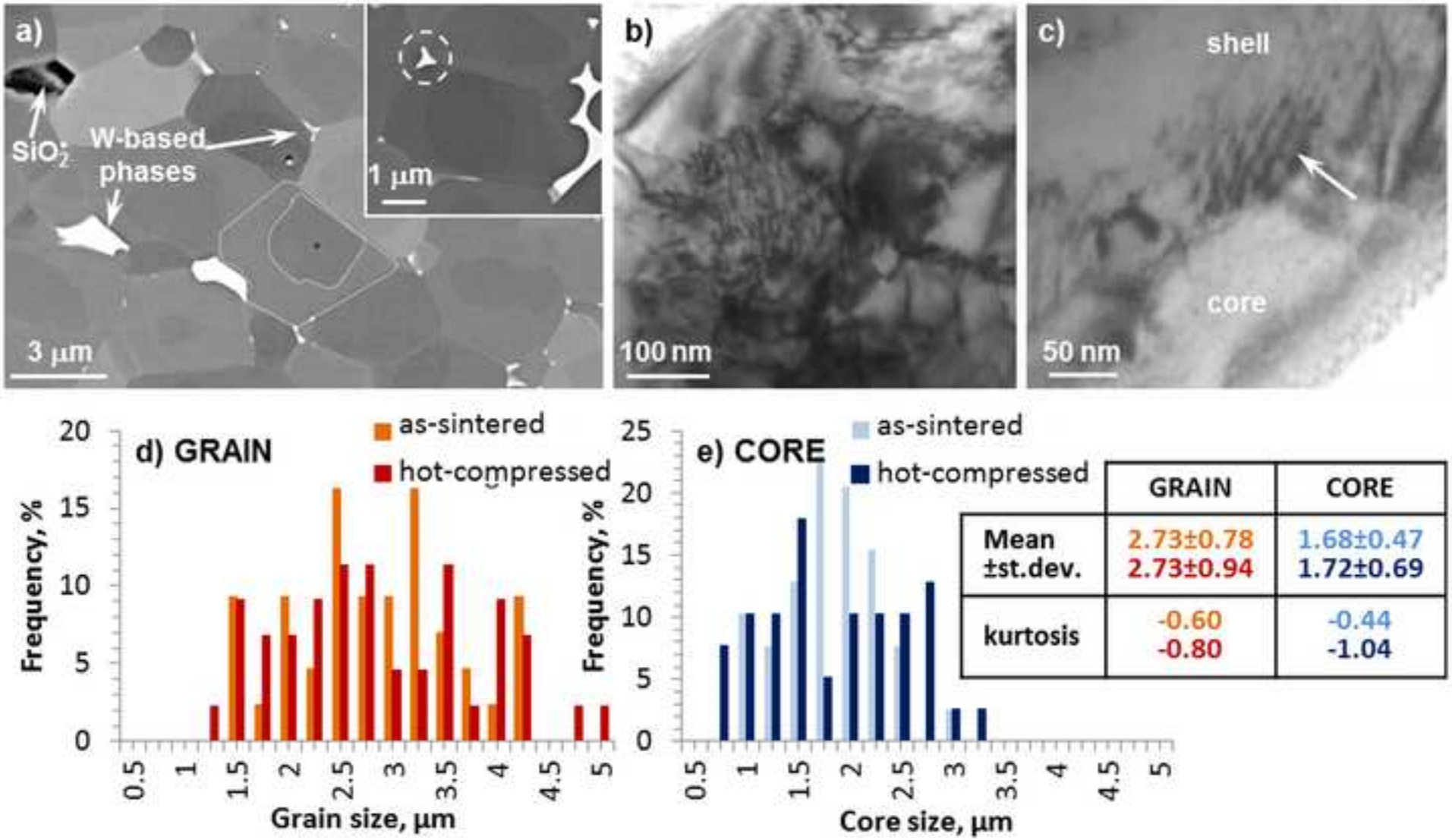

	GRAIN	CORE
Mean ±st.dev.	2.73±0.78 2.73±0.94	1.68±0.47 1.72±0.69
kurtosis	-0.60 -0.80	-0.44 -1.04

Figure 4

Click here to download high resolution image